ELSEVIER

Contents lists available at ScienceDirect

Chaos, Solitons and Fractals

journal homepage: www.elsevier.com/locate/chaos





Stochastically drifted Brownian motion for self-propelled particles

Dipesh Baral^a, Annie C. Lu^a, Alan R. Bishop^b, Kim Ø. Rasmussen^b, Nikolaos K. Voulgarakis^{a,*}

- ^a Department of Mathematics and Statistics, Washington State University, Pullman, WA 99164, USA
- ^b Theoretical Division, Los Alamos National Laboratory, Los Alamos, NM 87545, USA

ARTICLE INFO

Keywords: Active Brownian motion Transient superdiffusion Self-propelled particles Heterogeneous environments

ABSTRACT

Brownian Motion, with some persistence in the direction of motion, typically known as active Brownian Motion, has been observed in many significant chemical and biological transport processes. Here, we present a model of drifted Brownian Motion that considers a nonlinear stochastic drift with constant or fluctuating diffusivity. The interplay between nonlinearity and structural heterogeneity of the environment can explain three essential features of active transport. These features, which are commonly observed in experiments and molecular dynamics simulations, include transient superdiffusion, ephemeral non-Gaussian displacement distribution, and non-monotonic evolution of non-Gaussian parameter. Our results compare qualitatively well with experiments of self-propelled particles in simple hydrogen peroxide solutions and molecular dynamics simulations of self-propelled particles in more complex settings such as viscoelastic polymeric media.

1. Introduction

During the early 1900s, Brownian Motion (BM) was established as a stochastic process with two fundamental properties [1–3]. First, the position of the Brownian particle is characterized by a Gaussian distribution, and second, the mean square displacement (MSD) increases linearly with time. However, exceptions to these properties were observed as early as 1926 when Richardson [4] reported that the MSD of two tracer particles in a turbulent flow was proportional to the third power of time (MSD \propto t^3). Such observations of anomalous diffusion were reported frequently in subsequent years [5], leading to the characterization of anomalous diffusion by the following MSD relation

$$\langle R_{\star}^2 \rangle \propto t^{\rm v}$$
 (1)

where R_t is the position of the particle from the initial condition and $\langle \cdot \rangle$ represents the ensemble average. Here, ν is a non-negative exponent that indicates subdiffusion for $\nu < 1$, superdiffusion for $\nu > 1$, and Fickian diffusion for $\nu = 1$.

Our work focuses exclusively on active motion, typically characterized by $\nu \geq 1$ (see two excellent reviews [6,7]). Frequently, such superdiffusion occurs only transiently between two Fickian regimes at short and long time scales. Additionally, transient superdiffusion is very often characterized by a non-Gaussian probability density function (PDF) [8–14]. A commonly used metric to detect deviations from Gaussian distributions is the non-Gaussian parameter (NGP), which is directly related to the kurtosis of a PDF. In fact, NGP is simply one-third

of the excess kurtosis. However, because most experimental studies on anomalous diffusion utilize the NGP, we prefer to use it instead of kurtosis for easy comparison. Here, the NGP is used to specifically detect deviations from the Gaussian PDF of standard BM. In this context, all BMs have an NGP of zero. Examples of negative non-monotonic NGP have been observed in experiments involving self-propelled Janus particles in hydrogen peroxide (H_2O_2) solutions [14]. However, when the active particle is immersed in a more heterogeneous environment, such as viscoelastic polymeric suspensions, the NGP can be either purely positive or exhibit both positive and negative values, depending on the environment's heterogeneity [15]. Although not studied here, it is worth mentioning that nonmonotonic NGP has also been observed in systems exhibiting Fickian diffusion or transient subdiffusion (see, for example, [16–18]).

Persistent random walk (PRW) [19] and continuous time random walk (CTRW) [20] are two fundamental stochastic processes for modeling superdiffusion. The motion in PRW is characterized by the bias in a specific direction, whereas the particle dynamics in CTRW is described by the distribution of their displacement steps and waiting times [19,21–23]. Transient superdiffusion is possible when these distributions follow a power law [24] or tempered power-law distribution [25–27]. However, PRWs and CTRWs lack a straightforward way to describe the non-monotonic NGP and to incorporate external energy sources [27], two necessary components for active BM. A simple model that accommodates external energy sources to study active BM is the (fractional) Fokker–Planck equation [27,28], but an analytical solution of (fractional) Fokker–Planck equations is obtained only

E-mail address: n.voulgarakis@wsu.edu (N.K. Voulgarakis).

^{*} Corresponding author.

for a few special cases. From a microscopic perspective, generalized Langevin equation [29,30] using tempered or non-tempered memory kernels [31–35] scaled BM, [36,37], parabolic potential [38], non-linear friction function [39], and fractional derivatives [40] are used to model active BM. A basic generalized Langevin equation, popular as the active Ornstein–Uhlenbeck (OU) process, is achieved by using a colored Gaussian noise with exponentially decaying correlations [41]. Similarly, the addition of a potential leading to an extra acceleration term corresponds to the model of active BM, where particles take energy from the environment and store it in their internal energy depots [42]. A modified Langevin equation with additional telegraphic noise has been shown to produce transient superdiffusion [33].

In this work, we propose a simple model of drifted BM (dBM) with stochastic drift to describe active transport in heterogeneous environments. Although initially used to describe foraging dynamics [43], this model has the potential to explain three key characteristics of active BM. First, following [43–45], we demonstrate that the model can describe transient superdiffusion. Specifically, the MSD profile is Fickian at short times, superdiffusive at intermediate times, and returns to Fickian at longer times. Second, we have conducted numerical computations of the PDF and the NGP to demonstrate the non-Gaussian characteristics of active BM. These signatures are closely associated with experimental findings in active BM [8–14,46]. Third, the NGP shows the desired non-monotone behavior. By considering stochastic diffusivities that are commonly used to model heterogeneous environments [47–49], we show that the NGP exhibits further nontrivial behavior.

The paper is organized as follows. In Section 2, we present our model and define the measurables of this study. Section 3 presents the results of our simulation study and various properties of transient anomalous superdiffusion explained by the model. Specifically, Section 3.1 presents the results with constant diffusivities, while Section 3.2 uses the concept of fluctuating diffusivity. We end the paper with a brief summary in Section 4.

2. Model and measurables

Consider a particle moving in a complex n-dimensional (nd) environment described by two independent white noises $d\mathbf{B}_t^{(i)} = \sqrt{2D_i}d\mathbf{W}_t^{(i)}$, where $i=1,2,\ D_i$ are the corresponding diffusivities, and $\mathbf{W}_t^{(i)}$ denote n-dimensional independent Wiener processes. Here, we assume that the position of a particle, \mathbf{X}_t , under the influence of two distinct sources of noise can be modeled by the following stochastic differential equation,

$$d\mathbf{X}_{t} = \gamma \frac{\mathbf{B}_{t}^{(2)} - \mathbf{X}_{t}}{\|\mathbf{B}_{t}^{(2)} - \mathbf{X}_{t}\|} dt + d\mathbf{B}_{t}^{(1)}$$
(2)

where $\|\cdot\|$ is the Euclidian norm and γ is the drift velocity [43,44]. Qualitatively, this equation is easier to understand in 1d. In this case, the equation of motion reduces to

$$dX_{t} = \gamma \operatorname{sgn}(B_{t}^{(2)} - X_{t})dt + dB_{t}^{(1)},$$
(3)

where $sgn(\cdot)$ represents the standard sign function.

The first term in Eq. (3) describes the drift of the active particle. The particle moves with constant velocity in a specific direction (ballistic motion) until the difference $B_t^{(2)} - X_t$ changes sign. At that moment, the particle starts moving in the opposite direction until the next sign change. Let us call the distance between the two consecutive sign changes "flight". Since the sign changes are random, the length of these flights is also random. In the long term, the particle is trapped around $B_t^{(2)}$, and consequently, it exhibits behavior similar to $B_t^{(2)}$. The second term represents the random collisions of the active particle with the surrounding molecules. In the absence of any drift ($\gamma = 0$), the second term simply describes the BM of the tracer. In the short term ($t \to 0$) and before the first sign change, $X_t \approx \pm \gamma t + B_t^{(1)}$. Computing

the ensemble average of $(X_t - X_0)^2$ yields $MSD \approx \gamma^2 t^2 + 2D_1 t$. As the quadratic term becomes negligible when t approaches zero, $MSD \approx 2D_1 t$. This suggests that in the short term, the tracer behaves as $B_t^{(1)}$. In summary, the tracer behaves like $B_t^{(1)}$ in the short term, and in the long term, it adapts to the motion of $B_t^{(2)}$. Another interesting property of Eq. (3) is that the difference $u_t = B_t^{(1)} - X_t$ is effectively described by: $du_t = -\gamma \text{sgn}(u_t) + \sigma dW_t$, where $\sigma = \sqrt{2(D_1 + D_2)}$. This is simply the Langevin equation with dry friction equation first introduced by de Gennes [50]. The analytical solution, which is detailed in [51], possesses a Laplacian stationary distribution. These properties of the 1d model are qualitatively preserved in 2d and 3d. However, deriving them analytically is more challenging [43].

The model is characterized by three parameters: the two diffusivities $(D_1 \text{ and } D_2)$ and the drift (γ) . The surrounding fast molecules determine the value of the first diffusivity, D_1 , while the second diffusivity is related to the inevitable directional change of the particle's long flights. This directional change, and as a consequence, D_2 , depends on the strength of self-propulsion, the tracer's size and geometry, the mechanical properties of the environment, and tracer-environment interaction [15]. The drift velocity (γ) determines the onset of transition of the tracer from $B_t^{(1)}$ to $B_t^{(2)}$. These three parameters can be considered constant when active motion occurs in a simple environment, such as hydrogen peroxide. In cases where the active particle is immersed in environments exhibiting some dynamic or structural heterogeneity (e.g., polymeric suspensions), one can assume that these parameters are random variables or stochastic processes.

To model the effect of heterogeneous environments, this study assumes that only D_2 fluctuates in time. This process is called fluctuating or diffusive diffusivity [47–49,52]. To create a non-Gaussian process with non-monotone NGP, one needs to model the fluctuations of D_2 as a stochastic process with a stationary distribution. This process should change slowly over time, compared to the observation time scale of the particle's diffusion. For simplicity, we will implement the original fluctuating diffusivity approach that models $D_2(t)$ as

$$D_2(t) = \langle D_2(t) \rangle y_t^2, \tag{4}$$

where y_t is an OU process

$$dy_t = -\lambda y_t + \beta dW_t. ag{5}$$

Here, λ is the relaxation parameter, and β represents the white noise variance of the standard OU process. The mean, variance, and autocorrelation of y_t are $\langle y_t \rangle = 0$, $\langle \delta y_t^2 \rangle = \beta^2/2\lambda$ and $\langle y_t y_{t'} \rangle = (\beta^2/2\lambda)$ exp $(-\lambda|t-t'|)$, respectively. Eq. (4) implies $\langle \delta y_t^2 \rangle = 1$. Under these assumptions, the behavior of $D_2(t)$ is controlled by the relaxation parameter λ . In that case, the second BM that modulates the stochastic drift of the active particle is given by $\mathbf{B}_t^{(2)} = \int_0^t \sqrt{2D_2(s)}d\mathbf{W}_s^{(2)}$. As demonstrated in [44] and discussed below, stochastic diffusivity models can describe Fickian or transient anomalous diffusion with non-Gaussian PDF.

It should be emphasized that the analytical solution of Eq. (2) is not known yet and, therefore, will be solved numerically following the approach detailed in [43].

In this work, we will examine three main properties of the system. First, we compute the MSD of the tracer's position from the initial condition, i.e., $\langle \mathbf{R}_t^2 \rangle$, where $\mathbf{R}_t = \mathbf{X}_t - \mathbf{X}_0$. Second, we analyze the PDF of $R_{\alpha,t}$, $P(R_{\alpha,t})$, where $\alpha=1,2$, or 3 indicates the three different dimensions. The PDF is computed using the van Hove function [53]. Third, we demonstrate deviations from the Gaussian PDF of BM by calculating the NGP $a_2(t) = \langle R_{\alpha,t}^4 \rangle/(3\langle R_{\alpha,t}^2 \rangle) - 1$. We reiterate that the NGP is simply one-third of the excess kurtosis and is zero for a pure BM. To simplify the discussion of our results, we characterize positive NGP values as typically associated with PDFs having narrower peaks and broader tails (leptokurtic), while negative NGP values with PDFs that have flatter peaks and narrower tails (platykurtic). These PDF tails can be either Gaussian or non-Gaussian. However, it is important to

emphasize that we do not intend to generalize such characterization of positive and negative NGP. We underline that kurtosis gives a more elegant picture of a PDF than just its top flatness or tail heaviness [54].

Eqs. (2) and (3) have been studied in [43] in the context of animal foraging. It was shown that (a) the model exhibits transient superdiffusion, (b) the time of the particle's flights is distributed as an inverse Gaussian, and (c) the relaxation of the drift autocorrelation function is non-exponential. Here, we extend this study and demonstrate that the model can capture the enhancement of diffusivity and the non-monotonic behavior of the NGP often observed in active motion. Eq. (3) with a linear drift was studied in [44,45] and showed that it also exhibits transient anomalous diffusion. However, this nonlinearity is essential because, as we will see below, it enables our model to capture the negative NGP of self-propelled particles.

3. Transient superdiffusion with non-Gaussian characteristics

3.1. Constant diffusivities

Let us start our analysis by presenting the results for constant D_2 . This case can describe self-propelled particles in relatively simple fluidic environments. As we will see below, our model agrees very well with experimental and theoretical studies of Janus particle transport in hydrogen peroxide solutions [14]. Fig. 1 presents an example demonstrating our model's main properties. The parameters used in this example are $D_1=0.1$ and $\gamma=1$. The second diffusivity takes three different values $D_2=D_1$, $D_2=10D_1$, and $D_2=100D_1$.

The MSD profiles for the three different values of D_2 are shown in Fig. 1a. Note that the two vertical lines at τ_1 and τ_2 define three regions that reveal two important characteristics of our model. First, the MSD starts as diffusive with diffusivity D_1 (region I) and entails being also diffusive with diffusivity $D_2 \ge D_1$ (region III). Thus, our model can effectively capture the enhanced diffusivity of self-propelled particles that is commonly observed in active BM. For example, when Janus particles are immersed in a H2O2 solution, their diffusivity is enhanced by increasing the concentration of H2O2 [14]. In our model, this diffusion enhancement is regulated by D_2 . Second, the behavior of the MSD in the second time region (II) is unavoidably superdiffusive as long as $D_2 > D_1$ and is diffusive only if $D_2 = D_1$. Our model thus describes the transient superdiffusion associated with diffusivity enhancement. The exponent of superdiffusion ν is determined by the difference $D_2 - D_1$. Specifically, the exponent increases from $\nu = 1$ to approximately $\nu = 2$ with increasing $D_2 - D_1$. Furthermore, the parameter γ controls when the system enters the anomalous diffusion regime (Section 2). A small γ delays the time the MSD starts to enter the anomalous range, i.e., increases the value of τ_1 and τ_2 while a large γ decreases the value of τ_1 and τ_2 essentially pushing the system to Section 3's linear diffusive regime early. Also, $\gamma = 0$ reduces the system to standard BM, $\mathbf{B}_{t}^{(1)}$. It has to be mentioned that if $D_{2} < D_{1}$, the model describes transient subdiffusion associated with trapping events due to dynamic or structural heterogeneity [44].

Fig. 1b illustrates the NGP of the active particle for the three different values of D_2 . Note that for $D_2 = D_1$ (green circles), $a_2 = 0$, which means that the process is pure BM. For $D_2 > D_1$, the NGP is non-monotonic and takes only negative values. Specifically, the NGP is zero for $t < \tau_1$, then it starts decreasing at time τ_1 , reaches its minimum point, and then gradually becomes zero again at a relatively larger time. As D_2 increases, the non-Gaussianity becomes more prominent. Remarkably, this type of non-monotonic NGP has been observed, both experimentally and theoretically, in active Janus particles with transient superdiffusive behavior [14]. It is emphasized that our model can describe negative non-monotonic NGP due to the nonlinear nature of the drift. Linear drifts, such as those presented in [44,45], result in Gaussian processes.

As mentioned in the introduction, negative values of a_2 correspond to platykurtic distributions. A convenient way to display deviations

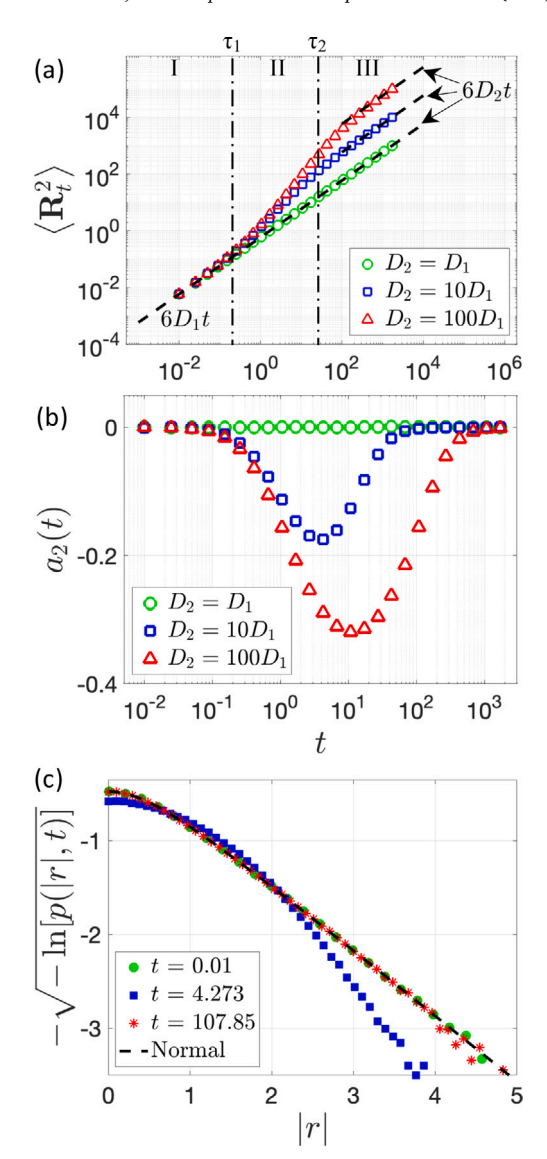


Fig. 1. Transient superdiffusive and non-Gaussian dynamics. In all subfigures, $D_1=0.1$ and $\gamma=1$. Panel (a) presents the MSD for $D_2=D_1$ (green circles), $D_2=10D_1$ (blue squares), and $D_2=100D_1$ (red triangles). In (a), dashed black lines represent the indicated linear MSD profiles, and the two vertical lines highlight the times τ_1 and τ_2 that separate the profile in the regions I (diffusion), II (superdiffusive), and III (diffusion). The superdiffusion regime is characterized by $\nu\approx1.75, 1.5$, and 1 for $D_2=100D_1, 10D_1, \text{ and } D_1, \text{ respectively. Panel (b) shows the corresponding NGP for the same three parameter sets as in panel (a). Panel (c) illustrates the PDF of the tracer for <math>D_2=10D_1$ at times t=0.01 and t=4.273 and t=107.85. The black dashed line corresponds to the standard normal. (For interpretation of the references to color in this figure legend, the reader is referred to the web version of this article.)

from a Gaussian PDF is by comparing the PDFs of the tracer at different times after rescaling $r=R_{\alpha,l}/\sqrt{\left\langle R_{\alpha,l}^2\right\rangle}$ [55]. To ensure that the normalization condition is satisfied, we rescale the PDF as $p(|r|,t)=P(|R_{\alpha,l}|,t)\sqrt{\left\langle R_{\alpha,l}^2\right\rangle}$. In a zero mean case like ours, all Gaussian distributions collapse to the standard normal $G(|r|)=\sqrt{2/\pi}\exp(-r^2/2)$. Deviations from the standard normal are easier detected by plotting $-\sqrt{-\ln(p(|r|,t))}$ versus |r|. In this representation, the tails of normal distributions are linear. Fig. 1c depicts the rescaled PDF of the tracer's position for $D_2=10D_1$ at three different times: t=0.01, 4.273, and 107.85, which belong to the three different diffusive regimes (see Fig. 1a), respectively. All three distributions are compared directly with the standard normal represented by the black dashed curve. It is clear

that the rescaled PDF matches the standard normal for short and long-term regimes, t = 0.01 and t = 107.85, respectively. These two Gaussian distributions reside in the Fickian regions I and III of the MSD presented in Fig. 1a. In practice, the tracer behaves like $\mathbf{B}_t^{(1)}$ for short times and adapts to the dynamics of $\mathbf{B}_t^{(2)}$ at long times. In the intermediate time, t = 4.273, the distribution deviates from the standard Gaussian distribution as it is more flattened at the top and more compact at the tails (platykurtic). This flattened distribution results from the tracer's ballistic motion as it approaches $\mathbf{B}_t^{(2)}$.

Overall, the results presented in this section agree qualitatively with the experiment of self-propelled Janus particles reported in [14].

3.2. Fluctuating diffusivities

Next, we will discuss the case of fluctuating diffusivities. This extension of our model is quite promising for active motion in environments that exhibit structural heterogeneity, such as biological soft matter or suspensions of polymeric chains. Such environments create trapping events that could lead to leptokurtic PDFs. Modeling this type of structural heterogeneity with OU-type stochastic diffusivity results in a positive NGP accompanied by leptokurtic PDFs [44,47–49,52]. It is expected that the interplay between entrapment (leptokurtic PDF) and active motion (platykurtic PDF) will ultimately shape the PDF of the tracer. As we will see below, by tuning the relaxation parameter (λ) of the OU process, we were able to qualitatively reproduce molecular dynamics (MD) simulation results of self-propelled particles in polymeric media [15].

Here, we kept the values of D_1 and γ the same as in the previous section. The average value of the second diffusivity was set to $\langle D_2(t) \rangle = 10D_1$. We studied two cases of fluctuating diffusivity, one for $\lambda=0.2$ and another for $\lambda=0.02$. Figs. 2a and 2b display the MSD and NGP, respectively, for the two values of lambda. For comparison purposes, we also include the case of constant $D_2=10D_1$ (see blue squares in Figs. 1a and 1b). As shown in Fig. 2a, the MSD of the tracer is not significantly affected by fluctuating diffusivity. It appears that the exponent ν is slightly decreased when compared to the constant diffusivity case. However, the impact of fluctuating diffusivity on the NGP is rather drastic. For the higher value of $\lambda=0.2$, the NGP exhibits a peculiar behavior. Initially, it takes negative values, and after a certain time ($t\approx10$), it becomes positive. Interestingly, decreasing to $\lambda=0.02$ eliminates negative values, resulting in a solely positive NGP.

This striking shift in the behavior of the NGP can be explained by the tracer's PDF profiles. To better understand the analysis below, we need to recall that for constant D_2 , the NGP is negative (blue squares in Fig. 2b) for times $t_1 < t < t_2$, where $t_1 = 0.05$ and $t_2 = 107.945$. The maximum negative value of the NGP is at time $t_{\rm m}=4.273$. In Fig. 2c, we display the PDF of the tracer for $\lambda = 0.2$ at t_1 , $t_{\rm m}$, and t_2 . At t_1 , the NGP is zero, resulting in normal PDF (green circles in Fig. 2c). As time progresses to $t_{\rm m}$, active motion dominates entrapment, leading to an overall negative NGP with a platykurtic PDF (see blue squares in Fig. 2c). Over time, the entrapment effect gradually increases, and for t > 10, the NGP becomes positive giving the tracer a leptokurtic PDF. This is clearly seen in Fig. 2c (red triangles), where we plot the PDF at time t_2 . Fig. 2d shows the tracer's PDFs for $\lambda = 0.02$ at the times t_1 , t_m , and t_2 . For the same reasons as in Fig. 2c, the PDF at time t_1 is normal, and the PDF at time t_2 is leptokurtic. Although the NGP for $\lambda = 0.02$ is positive at $t_{\rm m}$ (see magenta triangles in Fig. 2b), the PDF is not purely leptokurtic. It does have a leptokurtic structure up to $r \approx 3$, after which the tails become slightly narrower compared to a normal distribution. This narrowing, however, is not significant enough to give a negative overall value to the NGP. This PDF is an interesting example of a distribution with positive NGP (or excess kurtosis) that has a tail narrower than the normal distribution.

This type of nontrivial NGP behavior has been reported in MD simulations of self-propelled particles in polymeric suspensions [15]. By adjusting the parameters of the model, the authors of [15] were able

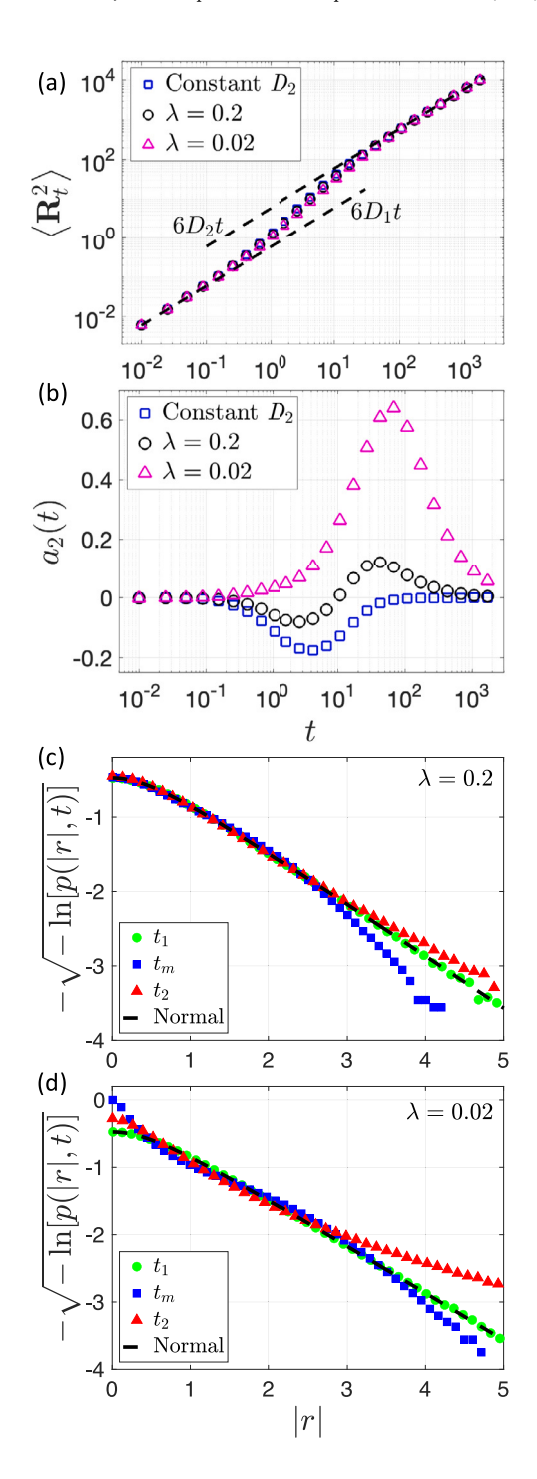


Fig. 2. The effect of stochastic diffusivity. In all subfigures, $\gamma=1$, $D_1=0.1$, and $\langle D_2(t)\rangle=10D_1$. Panel (a) and (b) show the MSD and the NGP, respectively, for $\lambda=0.2$ (black circles) and $\lambda=0.02$ (magenta triangles). For comparison reasons, the corresponding results from Figs. 1a and 1b for constant $D_2=10D_1$ are also presented (blue squares). Panels (c) and (d) show the tracer's PDF for $\lambda=0.2$ and $\lambda=0.02$, respectively, at three different times, $t_1=0.05$, $t_m=4.273$, and $t_2=107.945$, in comparison with the standard normal (red line). (For interpretation of the references to color in this figure legend, the reader is referred to the web version of this article.)

to effectively change the environment's heterogeneity. It was observed that when the particle had high polymer-tracer interaction and low self-propulsion force, the impact of the environment increased, resulting in a positive non-monotonic NGP, similar to the magenta triangles shown in Fig. 2b. On the other hand, when the particle had low interaction and

high propulsion force, it was able to navigate through the polymeric suspension more easily, effectively reducing the heterogeneity of the environment. In such cases, the NGP was negative non-monotonic, as represented by the blue squares in Fig. 2b. Intermediate values of propulsion force showed a non-monotonic behavior with both negative and positive values, as indicated by the black circles in Fig. 2b. These results are directly comparable to our predictions. In our model, the heterogeneity of the environment increases with decreasing the relaxation parameter λ . In practice, this adjustment reduces the response rate of the stochastic diffusivity.

4. Conclusions

This study presented a simple dBM equation with nonlinear stochastic drift to describe the dynamics of self-propelled particles. To account for structural heterogeneity in the fluidic environment, we used the concept of stochastic diffusivities. Numerical simulations showed that the interplay between non-linearity and heterogeneity can explain three important properties of active transport: transient superdiffusion and non-Gaussian PDF with non-monotonic NGP. Our model can describe both negative and positive NGP and their combinations. These results agree well with experiments of self-propelled Janus particles in relatively simple hydrogen peroxide solution [14], as well as with simulations of self-propelled particles in more complex settings such as polymeric melts [15]. Additionally, the striking similarity between our results and the dynamics of actively driven polymers [56] suggests that our model could be applied to polymer sorting in active fluids.

CRediT authorship contribution statement

Dipesh Baral: Writing – review & editing, Writing – original draft, Visualization, Validation, Software, Formal analysis, Data curation. **Annie C. Lu:** Validation, Software, Investigation, Formal analysis. **Alan R. Bishop:** Writing – review & editing, Investigation, Formal analysis. **Kim Ø. Rasmussen:** Writing – review & editing, Investigation, Formal analysis. **Nikolaos K. Voulgarakis:** Writing – review & editing, Writing – original draft, Visualization, Validation, Supervision, Software, Methodology, Investigation, Formal analysis, Data curation, Conceptualization.

Declaration of competing interest

The authors declare that they have no known competing financial interests or personal relationships that could have appeared to influence the work reported in this paper.

Data availability

Data will be made available on request.

Acknowledgments

DB, ACL, and NKV acknowledge support from the National Science Foundation, United States under Grant No. 1951583.

References

- Einstein A. Über die von der molekularkinetischen theorie der wärme geforderte bewegung von in ruhenden flüssigkeiten suspendierten teilchen. Ann Phys, Lpz 1905-17-132-48
- [2] Smoluchowski Mv. Zur kinetischen theorie der brownschen molekular bewegung und der suspensionen. Ann d Phys 1906;21:756–80.
- [3] Langevin P. Sur la théorie du mouvement brownien [On the Theory of Brownian Motion]. C R Acad Sci Paris 1908;146:530–3.
- [4] Richardson LF. Atmospheric diffusion shown on a distance-neighbour graph. Proc R Soc Lond Ser A 1926;110(756):709–37.

- [5] Metzler R, Jeon JH, Cherstvy AG, Barkai E. Anomalous diffusion models and their properties: Non-stationarity, non-ergodicity, and ageing at the centenary of single particle tracking. Phys Chem Chem Phys 2014;16:24128–64. http: //dx.doi.org/10.1039/c4cp03465a.
- [6] Romanczuk P, Bär M, Ebeling W, Lindner B, Schimansky-Geier L. Active Brownian particles: From individual to collective stochastic dynamics. Eur Phys J Spec Top 2012;202(1):1–162.
- [7] Bechinger C, Di Leonardo R, Löwen H, Reichhardt C, Volpe G, Volpe G. Active particles in complex and crowded environments. Rev Modern Phys 2016;88(4):045006.
- [8] Cherstvy AG, Nagel O, Beta C, Metzler R, Non-gaussianity, heterogeneity population. And transient superdiffusion in the spreading dynamics of amoeboid cells. Phys Chem Chem Phys 2018;20:23034–54.
- [9] Dieterich P, Klages R, Preuss R, Schwab A. Anomalous dynamics of cell migration. Proc Natl Acad Sci 2008;105(2):459–63.
- [10] Thapa S, Lukat N, Selhuber-Unkel C, Cherstvy AG, Metzler R. Transient superdiffusion of polydisperse vacuoles in highly motile amoeboid cells. J Chem Phys 2019:150(14):144901.
- [11] Metzler R, Jeon J-H, Cherstvy A. Non-Brownian diffusion in lipid membranes: Experiments and simulations. Biochim Biophys Acta (BBA)-Biomembranes 2016;1858(10):2451–67.
- [12] Kurtuldu H, Guasto JS, Johnson KA, Gollub JP. Enhancement of biomixing by swimming algal cells in two-dimensional films. Proc Natl Acad Sci 2011;108(26):10391-5.
- [13] Charbonneau P, Jin Y, Parisi G, Zamponi F. Hopping and the Stokes– Einstein relation breakdown in simple glass formers. Proc Natl Acad Sci 2014;111(42):15025–30.
- [14] Zheng X, Ten Hagen B, Kaiser A, Wu M, Cui H, Silber-Li Z, Löwen H. Non-gaussian statistics for the motion of self-propelled janus particles: Experiment versus theory. Phys Rev E 2013;88(3):032304.
- [15] Yadav RS, Das C, Chakrabarti R. Dynamics of a spherical self-propelled tracer in a polymeric medium: interplay of self-propulsion, stickiness, and crowding. Soft Matter 2023:19:689–700.
- [16] Wang B, Kuo J, Bae SC, Granick S. When Brownian diffusion is not Gaussian. Nature Mater 2012;11(6):481–5. http://dx.doi.org/10.1038/NMAT3308.
- [17] Wang B, Anthony SM, Sung CB, Granick S. Anomalous yet Brownian. Proc Natl Acad Sci USA 2009;106(36):15160-4. http://dx.doi.org/10.1073/PNAS. 0903554106.
- [18] Chakraborty T, Pradhan P. Time-dependent properties of run-and-tumble particles. II. current fluctuations. Phys Rev E 2024;109:044135.
- [19] Fürth R. Die brownsche bewegung bei berücksichtigung einer persistenz der bewegungsrichtung. mit anwendungen auf die bewegung lebender infusorien. Z Phys 1920;2(3):244–56.
- [20] Montroll EW, Weiss GH. Random walks on lattices. II. J Math Phys 2004;6(2):167–81.
- [21] Rubner O, Heuer A. From elementary steps to structural relaxation: A continuous-time random-walk analysis of a supercooled liquid. Phys Rev E 2008;78:011504.
- [22] Helfferich J, Ziebert F, Frey S, Meyer H, Farago J, Blumen A, et al. Continuous-time random-walk approach to supercooled liquids. II. mean-square displacements in polymer melts. Phys Rev E 2014;89(4):042604.
- [23] Jeon J-H, Barkai E, Metzler R. Noisy continuous time random walks. J Chem Phys 2013;139(12).
- [24] Song MS, Moon HC, Jeon J-H, Park HY. Neuronal messenger ribonucleoprotein transport follows an aging lévy walk. Nature Commun 2018;9(1):1–8.
- [25] Sabzikar F, Meerschaert MM, Chen J. Tempered fractional calculus. J Comput Phys 2015;293:14–28.
- [26] Zhang Y, Meerschaert MM, Packman AI. Linking fluvial bed sediment transport across scales. Geophys Res Lett 2012;39(20).
- [27] Metzler R, Klafter J. The random walk's guide to anomalous diffusion: a fractional dynamics approach. Phys Rep 2000;339(1):1–77.
- [28] Herrera P, Sandoval M. Maxwell-Boltzmann velocity distribution for noninteracting active matter. Phys Rev E 2021;103:012601.
- [29] Mori H. Transport, collective motion, and Brownian motion*). Progr Theoret Phys 1965;33(3):423–55.
- [30] Tokyo J. Summer Institute of theoretical physics. 1St, Oiso, R. Kubo, Many-body theory. Lectures edited by ryogo kubo, 1966.
- [31] Zwanzig R. Memory effects in irreversible thermodynamics. Phys Rev 1961;124(4):983.
- [32] McKinley SA, Nguyen HD. Anomalous diffusion and the generalized Langevin equation. SIAM J Math Anal 2018;50(5):5119–60.
- [33] Um J, Song T, Jeon J-H. Langevin dynamics driven by a telegraphic active noise. Front Phys 2019;7:143.
- [34] ten Hagen B, van Teeffelen S, Löwen H. Brownian motion of a self-propelled particle. J Phys: Condens Matter 2011;23(19):194119.
- [35] Peruani F, Morelli LG. Self-propelled particles with fluctuating speed and direction of motion in two dimensions. Phys Rev Lett 2007;99(1):010602.
- [36] Bodrova AS, Chechkin AV, Cherstvy AG, Safdari H, Sokolov IM, Metzler R. Underdamped scaled brownian motion:(non-) existence of the overdamped limit in anomalous diffusion. Sci Rep 2016;6(1):30520.

- [37] Safdari H, Cherstvy AG, Chechkin AV, Bodrova A, Metzler R. Aging underdamped scaled Brownian motion: Ensemble-and time-averaged particle displacements, nonergodicity, and the failure of the overdamping approximation. Phys Rev E 2017;95(1):012120.
- [38] Schweitzer F, Ebeling W, Tilch B. Complex motion of Brownian particles with energy depots. Phys Rev Lett 1998;80(23):5044.
- [39] Erdmann U, Ebeling W, Schimansky-Geier L, Schweitzer F. Brownian particles far from equilibrium. Eur Phys J B 2000;15:105–13.
- [40] Joo S, Durang X, c. Lee O, Jeon J-H. Anomalous diffusion of active Brownian particles cross-linked to a networked polymer: Langevin dynamics simulation and theory. Soft Matter 2020;16(40):9188–201.
- [41] Martin D, O'Byrne J, Cates ME, Fodor É, Nardini C, Tailleur J, Van Wijland F. Statistical mechanics of active Ornstein-Uhlenbeck particles. Phys Rev E 2021;103(3):032607.
- [42] Ebeling W, Schweitzer F, Tilch B. Active Brownian particles with energy depots modeling animal mobility. BioSystems 1999;49(1):17–29.
- [43] Toman K, Voulgarakis NK. Stochastic pursuit-evasion curves for foraging dynamics. Phys A 2022;597:127324.
- [44] Voulgarakis NK. Multilayered noise model for transport in complex environments. Phys Rev E 2023;108(16):064105.
- [45] Wang J, Voulgarakis NK. Hierarchically coupled Ornstein-Uhlenbeck processes for transient anomalous diffusion. Physics 2024;6(2):645–58.

- [46] De Bruin K, Ruthardt N, Von Gersdorff K, Bausinger R, Wagner E, Ogris M, et al. Cellular dynamics of egf receptor–targeted synthetic viruses. Molecular Therapy 2007:15(7):1297–305.
- [47] Chubynsky MV, Slater GW. Diffusing diffusivity: A model for anomalous, yet Brownian, diffusion. Phys Rev Lett 2014;113(9).
- [48] Chechkin AV, Seno F, Metzler R, Sokolov IM. Brownian yet non-Gaussian diffusion: From superstatistics to subordination of diffusing diffusivities. Phys Rev X 2017;7(2):021002.
- [49] Lanoiselée Y, Grebenkov DS. A model of non-Gaussian diffusion in heterogeneous media. J Phys A 2018;51(14):145602.
- [50] d. Gennes PG. Brownian motion with dry friction. J Stat Phys 2005;119:953–62.
- [51] Touchette H, Straeten EVD, Just W. Brownian motion with dry friction: Fokker-planck approach. J Phys A 2010;43.
- [52] Jain R, Sebastian KL. Diffusing diffusivity: Survival in a crowded rearranging and bounded domain. J Phys Chem B 2016;120(34):9215–22.
- [53] Van Hove L. Correlations in space and time and born approximation scattering in systems of interacting particles. Phys Rev 1954;95(1):249.
- [54] Kleiber C, Kotz S. Statistical size distributions in economics and actuarial sciences. John Wiley & Sons; 2003.
- [55] Pastore R, Ciarlo A, Pesce G, Greco F, Sasso A. Rapid Fickian Yet Non-Gaussian Diffusion after Subdiffusion. Phys Rev Lett 2021;126(15):158003.
- [56] Shin J, Cherstvy AG, Kim WK, Zaburdaev V. Elasticity-based polymer sorting in active fluids: A Brownian dynamics study. Phys Chem Chem Phys 2017;19(28):18338–47.